

Geoelectric Section of the Central Tien Shan: Sequential Inversion of the Magnetovariational and Magnetotelluric Data along the Naryn Line

M. N. Berdichevsky^{a†}, N. S. Golubtsova^a, Iv. M. Varentsov^b, P. Yu. Pushkarev^a,
A. K. Rybin^c, and E. Yu. Sokolova^b

^a Geological Faculty, Moscow State University, Moscow, 119991 Russia

^b Geoelectromagnetic Research Centre, Schmidt Institute of Physics of the Earth, Russian Academy of Sciences
(GEMRC IPE RAS), Troitsk, Moscow oblast, 142092 Russia

^c Scientific Station of the Russian Academy of Science, Bishkek, Kyrgyzstan

Received January 25, 2010

Abstract—The paper presents the results of 2D inversion of deep magnetotelluric (MT) and magnetovariational (MV) soundings along the Naryn Line. The method of partial (sequential) inversions is used. According to this method, at the first stage, magnetovariation responses are used for the localization of deep anomalies of electrical conductivity, and then the magnetotelluric sounding data are invoked to refine the structure of the host medium and the structural details in the upper part of the section. It is shown that this approach enables one to estimate the informativeness of separate components of the electromagnetic field, to reduce the distorting influence of the near-surface geoelectric inhomogeneities, and to increase the stability of the final solution of the inverse problem.

DOI: 10.1134/S1069351310080069

INTRODUCTION

The first experiments on the sequential interpretation of magnetotelluric (MT) and magnetovariational (MV) soundings in the Tien Shan date back to 1988–1990, when a team of scientists within the Electromagnetic expedition of the Institute for High Temperatures of the Russian Academy of Sciences and the Moscow State University constructed geoelectric sections along three profiles intersecting the folded mountain structures of the Central Tien Shan in the near-meridional direction. The construction of these cross-sections was based on the MV data, which in the low-frequency range were free from the distortions caused by near-surface inhomogeneities [Trapeznikov et al., 1997]. The data recorded by the digital electromagnetic prospecting system CES-2 at more than a hundred sounding points were analyzed. Model calculations were performed with the program based on the finite element method [Wannamaker et al., 1987], and the model parameters were chosen intuitively by hand. In that work, several dozens of models had to be tested until a good fit of the model to the observed data was attained. At the same time, the results of electromagnetic soundings were compared with the seismic tomography data. The comparison showed that the reduced electrical resistivity of crustal blocks correlates with the reduced seismic velocities and with the

increased attenuation of seismic waves, which testifies for the fluid nature of the coinciding geoelectric and seismic anomalies [Kissin and Ruzaikin, 1997].

In the following years, the electromagnetic observations in the Tien Shan were significantly expanded. At this time, new methods for computer-aided inversion appeared. For the interpretation of the accumulated data, a research team was organized. The team called the NARYN working group included scientists from the Bishkek Scientific Station of the Russian Academy of Sciences, from the GeoElectromagnetic Research Centre of Schmidt Institute of Physics of the Earth, Russian Academy of Sciences (GEMRC IPE RAS) and from Moscow State University. The main objectives of this working group were to construct the geoelectric section of the Central Tien Shan from the entire set of MT and MV data along the Naryn Line (which is the most representative profile in terms of the density of observations) and to improve the methodology for interpretation of the deep sounding data in quasi-2D media with a complex structure.

We intended to present the results obtained by the NARYN working group in three papers. The first work of this cycle [Berdichevsky et al., 2010] describes the results of the advanced structural analysis of the entire set of MT and MV responses obtained along the Naryn geotraverse within a wide range of periods. In that paper the distortions of these responses caused by the

†Deceased.

surface and the deep 3D inhomogeneities are evaluated, and the segments of the profile and the intervals of periods that are most favorable for 2D interpretation of the data are identified.

The present paper is the second work of the planned cycle. The purpose of the present paper is to construct a simple and at the same time stable blocky geoelectric model along the entire profile from the results of the long-period soundings only. In addition to the observations conducted with the CES-2 and Phoenix instruments, 19 deep five-component MT soundings in the interval of periods 0.1–40 100 s were carried out using the LIMS instrumentation (14 in the territory of Kyrgyzstan and five in northern China). The arrangement of the points of deep sounding is presented in the work [Berdichevsky, 2010].

It is worth noting that the method of sequential interpretation of MT and MV responses was intensively developed when constructing the geoelectric model of the Cascadia subduction zone in the course of the joint work of the scientists from Moscow State University, the Shirshov Institute of Oceanology of RAS, and the GeoElectromagnetic Research Center of IPE RAS under the EMSLAB international project. In these studies, in particular, the efficiency was demonstrated of the approaches to the interpretation of quasi-2D data, based on the sequential 2D inversions of their separate components with the priority given to the MV responses and the impedance phases [Varentsov et al., 1996; Vanyan et al., 1997; 2002]. The efficiency of the method of sequential partial inversions is shown on a number of model and practical examples in [Berdichevsky, et al., 2003] and further investigated in the monograph by Berdichevsky and Dmitriev [2009]. This method is based on the detailed account of the differences in the sensitivity of the responses of the electromagnetic field to deep and surface conductors. The process of inversion is subdivided into three stages. At the first stage, the inversion of the MV data (the components (Re , Im) of the tipper W_z) is conducted; at the second stage, the inversion of the longitudinal phases of impedance ϕ^{\parallel} is carried out; and at the third stage, the inversion of the transverse amplitude and phase data (ρ^{\perp} , ϕ^{\perp}) is performed.

It was important to apply this simple but very efficient method in the severe conditions of the Central Tien Shan and to obtain a reliable model as the basis for the subsequent more detailed solutions to the problem of 2D inversion of the joint MT/MV data ensemble [Sokolova et al., 2007; 2008] in the scope of the general approach presented in the works [Varentsov, 2002; 2007]. This study had a substantial foundation: in the work [Berdichevsky et al., 2003], the specificity of the application of the technique of sequential partial inversions for the interpretation of the synthetic data in the “Naryn”-type model has been already analyzed.

In the first part of the present paper, we show the results of the preliminary study of the data to be interpreted, which lie beyond the scope of the systematic analysis of their accuracy and dimensionality conducted in [Berdichevsky et al., 2010]. In the second part, the results of the inversion of the MV data (tipplers) with the aid of the smoothing REBOCC algorithm [Siripunvaraporn and Egbert, 2000] are described. In the most important third part of the work, we present a series of the geoelectric models yielded by sequential partial inversions according to the INV2D algorithm [Varentsov, 2002; 2007], first for the MV data and then for the different impedance components.

Unfortunately, M.N. Berdichevsky had passed away when the work on this manuscript was still far from complete. We realize that with his participation the presentation of the obtained results would have been more comprehensive, precise, and vivid.

1. PRELIMINARY ANALYSIS OF THE MT/MV DATA

Validity Test of the Impedance Dispersion Relations

Before we proceed to interpreting the data, it is necessary to estimate their quality and, in particular, to check whether the impedance dispersion relationships hold. The dispersion relations between the apparent electrical resistivity (ρ) and the impedance phase (ϕ) are valid in a 1D (horizontally layered) and 2D (in the case of H -polarization of the field) media [Weidelt, 1972; Berdichevsky and Dmitriev, 1991]. In the 2D case of E -polarization they are violated in rather rare situations such as a sounding in deep canyons and deep floor surveys in the region of the coast slope [Alekseev et al., 2009].

For 14 soundings on the Kyrgyz part of the profile, the accuracy of the fulfillment of the dispersion relations was examined: conversion of ρ into ϕ and vice versa was carried out for the data corresponding to the longitudinal and transverse polarization of the field. Since the measuring axes of the soundings are oriented along the geomagnetic meridian (the x axis is oriented northwards) and the latitude (the y axis is oriented eastwards), and the strike of the deep geoelectric structures is close to the latitudinal direction, the initial curves ρ_{xy} and ρ_{yx} were taken as the transverse and longitudinal curves, respectively. The calculations were performed using the computer program developed by Pokhotelov [Berdichevsky and Pokhotelov, 1997] in the interval of periods 1– 10^4 s. The dispersion relationships are fulfilled with acceptable accuracy for almost all the soundings considered, which is evident in Fig. 1, where the initial phases are compared with the phases recalculated from the apparent electrical resistivities. Discrepancies are observed only at long periods, which is due to the uncertainties in the data

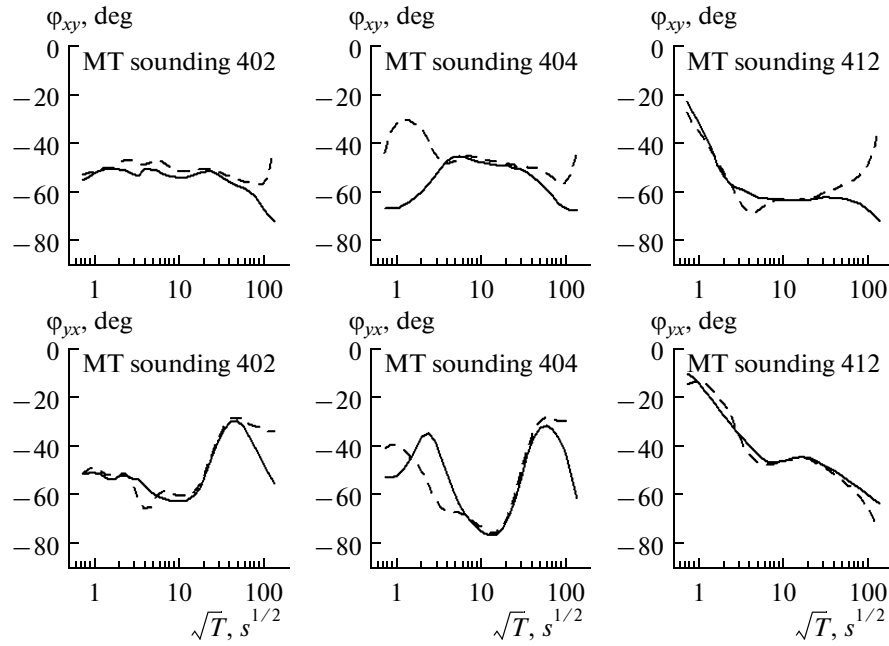


Fig. 1. Results of recalculations of the curves of apparent electrical resistivity into the phase curves for two field polarizations: the top row corresponds to the transverse polarization, the bottom row corresponds to the longitudinal polarization, the solid lines show the observed data, and the dotted lines show the calculated data.

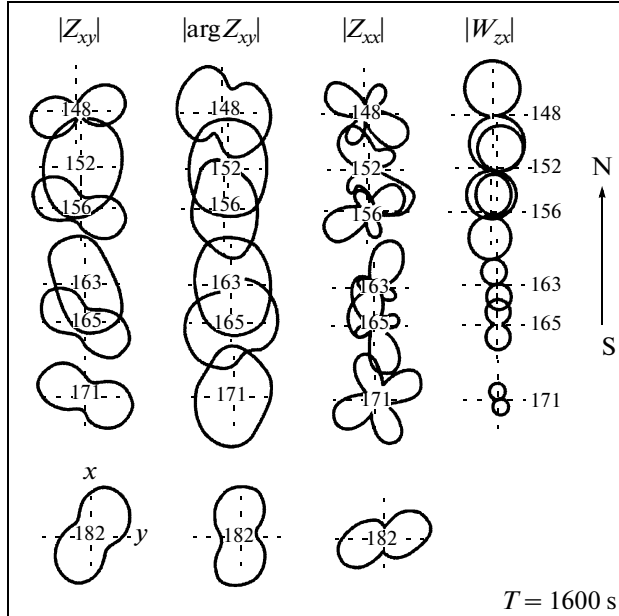


Fig. 2. Polar diagrams of impedance and tipper obtained from the CES-2 observations along the Naryn Line [Berdichevsky and Dmitriev, 2009], the numbers inside and near the polar diagrams designate the numbers of the sounding points.

extrapolation when calculating the dispersion integrals. Only at point 404, in periods up to 100 s, noticeable misfits between the observed and the calculated curves are observed.

Estimates of the Dimensionality and the Strike of Deep Structures

The detailed analysis of the invariant parameters of the MT/MV responses that characterize the dimensionality of the geoelectric medium and the strike of the predominant structures is carried out in [Berdichevsky et al., 2010]. Special attention was paid to obtaining estimates that are free from the distorting influence of near-surface inhomogeneities. It is shown that the impedance amplitudes experience strong static distortions throughout the entire range of periods. The longitudinal phases are substantially less distorted. The influence of sedimentary troughs on them, as a rule, is terminated at periods of a few hundreds of seconds. The analysis of the induction vectors and the parameters of asymmetry (skew) for the different MT/MV responses indicates that over the entire profile (especially in its northern part, points 405–414) the data exhibit rather stable quasi-two-dimensionality, which is complicated in some components and within particular sections of the profile by the static effects caused by the near-surface structures and by the upper-crustal 3D inhomogeneities.

We will expand this analysis by the examination of MT and MV polar diagrams, following the monograph [Berdichevsky and Dmitriev, 2009]. The polar diagrams of several components of the impedance and the tipper along the Naryn Line for the period of 1600 s are presented in Fig. 2. These diagrams are plotted according to the results of the early observations with

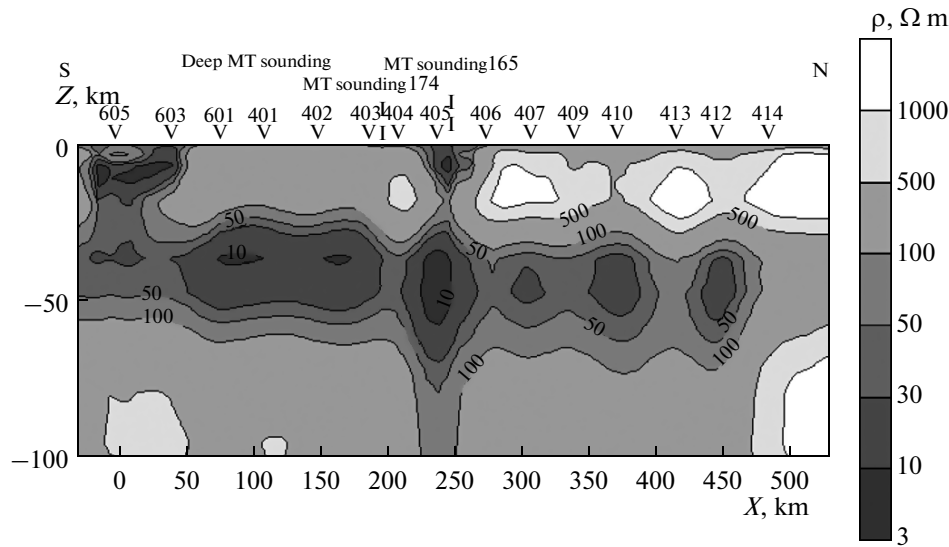


Fig. 3. Geoelectric section along the Naryn Line, from the results of inversion of the MV data (W_{zx}) with the aid of the REBOCC program; the contours of electrical resistivity are given in Ω m.

the CES-2 instrumentation and they serve as an additional demonstrative illustration to the basic conclusions of the work [Berdichevsky et al., 2010].

The impedance diagrams of $|Z_{xy}|$ and $|Z_{xx}|$ show no distinct regular pattern in the changes of the shape and orientation along the profile. The $|\arg Z_{xy}|$ diagrams are more immune to near-surface distortions. At many points they are elongated in the submeridional direction, following the near-latitudinal strike of the regional 2D structures. The amplitude diagrams of the tipper are most informative. At all points of the profile, the diagrams are eight-shaped with rather small waists; they are oriented in the near-meridional direction, which is distinctly indicative of latitudinally striking regional quasi-2D structures.

Thus, both the new long-period LIMS data and the old CES-2 data convincingly evidence that in the conditions of the Central Tien Shan the most informative components of the data (primarily, the MV responses and the impedance phases) can be interpreted quite well in the class of 2D models.

2. PRELIMINARY SMOOTHED 2D INVERSION OF MV DATA

Before conducting the sequential inversion in the block-type model, the smoothed 2D inversion of the long-period MV data was executed according to the REBOCC program [Siripunvaraporn and Egbert, 2000]. Here, our purpose was to show the informativeness of the tipper data W_{zx} with the minimal prior assumptions introduced in the parameterization scheme of the geoelectric model. In order to study the most interesting sections of the profile (the fault zone of the Nikolaev Line and the Atbashi-Inylchek fault)

in finer detail, the CES-2 data at points 165 and 174 were additionally invoked.

Two start models were examined: the uniform half-space and five-layer horizontally stratified model. In the layered model, the first layer modeled a sedimentary-volcanogenic cover ($\rho_1 \sim 100 \Omega$ m, $h_1 \sim 1$ km); the second layer reproduced a poorly conductive upper crust ($\rho_2 \sim 1000 \Omega$ m, $h_2 \sim 30$ km); the third layer represented a conductive crustal layer ($\rho_3 \sim 50 \Omega$ m, $h_3 \sim 25$ km); the fourth layer simulated a poorly conductive upper mantle ($\rho_4 \sim 500 \Omega$ m, $h_4 \sim 90$ km); and the fifth layer simulated a well conductive mantle ($\rho_5 = 50 \Omega$ m). The parameters of the layers are borrowed from the works [Trapeznikov et al., 1997; Berdichevsky and Dmitriev, 2002].

The calculations showed that if there is no conductive layer in the initial model, in the resultant model this layer does not form a unified continuous structure, but appears as several isolated spots. The most striking result was obtained in the inversion of the $\text{Re } W_{zx}$ component in the interval of periods from 25 to 1600 s with the horizontally layered medium used as the start model. The resultant geoelectric section down to a depth of 100 km is shown in Fig. 3. Here the crustal conductive layer that was discerned in the initial model at a depth of 30–60 km is imaged in much finer detail; it subsides from the south to the north and presumably thins out to the north of points 412–414. The layer is laterally inhomogeneous: the electrical resistivity decreases from the initial level of 50Ω m to below 10Ω m. Also, the conductive vertical zones are revealed, which connect the crustal conductor with the sedimentary cover. These zones are confined to the set of deep faults near point 405 (the Nikolaev Line), points 603–605 (the edge faults on the north of the Tarim Basin), and point 410 (the North Tien Shan

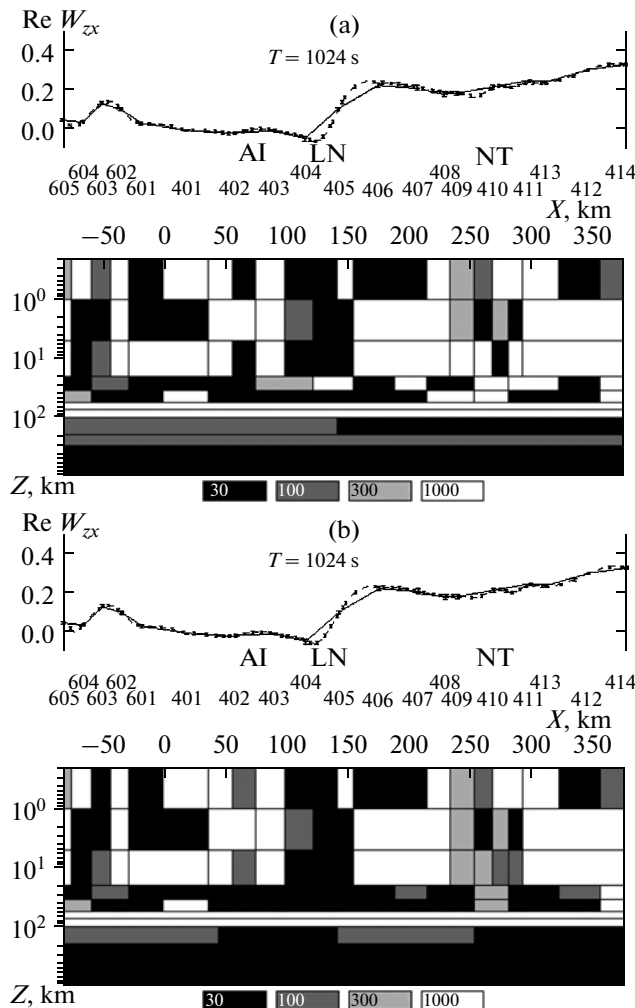


Fig. 4. Geoelectric model along the Naryn Line, according to the inversion of $\text{Re } W_{zx}$ and $\text{Im } W_{zx}$ using the INV2D program: (a) the initial solution, (b) the solution with the detailed representation of the upper mantle; at the top, the profile plots of the observed and model data are given for a period of 1024 s. Hereinafter the following designations are used: the solid line depicts the observed data, the dotted line depicts the model data, the numbers in the rectangles on the bottom designate the average value of the electrical resistivity of blocks in $\Omega \text{ m}$; AI stands for the Atbashi-Inylchek fault, LN stands for the Nikolaev Line, and NT stands for the North Tien Shan fault.

fault). It is important to emphasize that the tipper inversion not only localizes the deep anomalies of electrical conductivity, but also refines the layered structure of the host medium; in particular, an increase in the electrical resistivity of the upper crust from the Nikolaev Line northward is revealed.

3. SEQUENTIAL BLOCKY INVERSION OF MT/MV DATA

At this stage, a sequence of 2D inversions of MT/MV data is conducted in the class of blocky mod-

els with fixed geometry with the use of the INV2D algorithm [Varentsov, 2002; 2007]. In this algorithm, it is possible to choose different schemes of the model's parameterization; the scheme with the fixed geometry is the simplest one. When conducting a block type inversion, it is important that the size and the geometry of blocks are adequately specified. When constructing the interpretation model, we took into account the a priori data about the structure of the region and the results of the preliminary smoothed REBOCC inversion. The model was partitioned into blocks in accordance with the guidelines presented in [Dmitriev, 1987; Berdichevsky and Dmitriev, 1991; 2002]. The interpretation model, on the one hand, should reflect all the essential features of the section and, on the other hand, should be sufficiently simple to provide practical stability of the solution of the inverse problem. Therefore, the regions with expected sharp changes in the electrical conductivity were partitioned into blocks in greater detail, while the regions with slightly changing electrical conductivity were represented by the larger blocks. Thus, we obtained an initial model composed of 125 blocks, whose resistivities were to be optimized. The problems of modeling EM fields were solved on a finite-difference grid containing 90×44 nodes.

The MV and MT data in the obtained model was interpreted using the sequential partial inversions technique. The process of inversion includes four stages.

Inversion of MV Data ($\text{Re } W_{zx}$ and $\text{Im } W_{zx}$)

The initial model of inversion was a uniform half-space with an electrical resistivity of $1000 \Omega \text{ m}$. Partition of the model into blocks was carried out as follows. The modeling region in the Earth was divided into 10 layers; each of the 5 upper layers (down to a depth of 75 km) was divided into 23 blocks; the 2 next layers (down to a depth of 200 km) were divided into 4 blocks, and the lower basement (below 200 km) was composed of 2 blocks.

First of all, we had to determine the period starting from which the tipper becomes free from the influence of the near-surface inhomogeneities. The results of the structural analysis of MV responses, given in the first paper of the cycle [Berdichevsky et al., 2010], and also a number of tentative inversions for different intervals of periods, allowed us to infer that the best results characterized by the smallest misfits are obtained for the interval of periods 724–4096 s. In shorter periods, the influence of near-surface inhomogeneities remains essential, whereas in longer periods the effects of the heterogeneity of the external source appear.

The model obtained from the inversion of $\text{Re } W_{zx}$ and $\text{Im } W_{zx}$ is presented in Fig. 4a. We note that in this case with no a priori assumptions at all, the inversion of the MV responses alone recognizes all the main structural elements of the medium in the initial model

of the uniform half-space. The heterogeneous upper layer, which reproduces the sedimentary cover; four local conductive zones in the upper crust confined to the North Tien Shan fault (points 409–410), to the fault zone of the Nikolaev Line (point 405), to the Atbashi-Inylchek fault (point 403), and to the northern edge of the Tarim Basin (points 603–605); and the horizontally inhomogeneous crustal conducting layer at a depth of 20–55 km and a step in the asthenosphere at a depth 100–200 km below the Nikolaev Line are distinctly identified.

This model ensures quite satisfactory agreement between the model and the observed data in the entire interval of periods considered: the misfits do not exceed a few percent (Fig. 4a, top panel).

Some features of the constructed model seemed doubtful; therefore, we carried out two additional experiments.

Check for the Presence of Poorly Conductive Sectors in the Crustal Layer

The results of inversion showed that the conductive layer in the crust in some regions of the profile (under the Nikolaev Line and the North Tien Shan fault) contains high-resistivity blocks. In order to prevent a noticeable increase in the data misfits, attempts were made to replace the nonconductive blocks by those with higher conductivity, taking into account the equivalence principle. For eight blocks in the basement of the Nikolaev Line, the average electrical conductivity and the corresponding average electrical resistivity (ρ_{average}) were calculated; then, the values of resistivity of all the remaining blocks were fixed, and only these eight blocks were optimized ($\rho_{\text{initial}} = \rho_{\text{average}}$). The same procedure was applied to the blocks in the basement of the North Tien Shan fault.

The results showed that in the region of the Nikolaev Line, the poorly conductive blocks disappear; moreover, the total misfit of the model does not substantially increase, while the electrical resistivities at the basement of the North Tien Shan fault remain increased (100–200 Ω m). This result to some extent agrees with the conclusions of the paper [Trapeznikov et al., 1997] about the fact that in the northern part of the profile, the electrical resistivity of the crustal conductor increases, although in our model this increase cannot be called monotonic and smooth.

Check for the Presence of a Step in the Asthenosphere

The upper-mantle layer at a depth of 100–200 km was divided into a larger number of blocks than the amount of blocks in the initial model, and an inversion was carried out, in which the result of the previous inversion was taken as the initial model. This inversion revealed the lateral heterogeneity of the upper mantle containing conductive blocks that tend toward the ver-

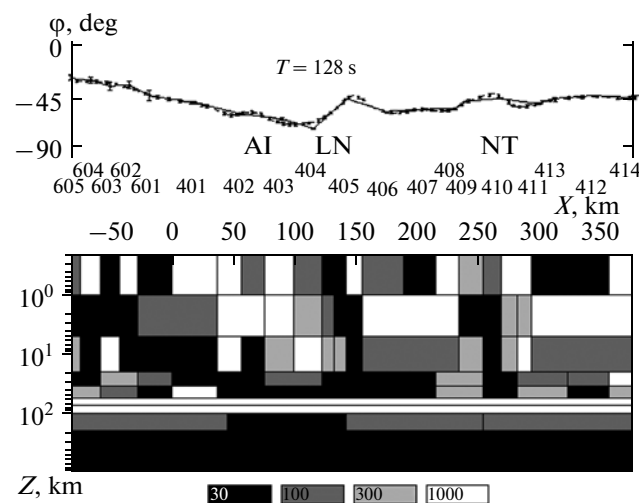


Fig. 5. Geoelectric model along the Naryn Line, constructed based on the results of inversion of longitudinal phases (the starting model is the result of inversion of tipplers); at the top, the profile plots of the observed and model longitudinal phases are presented for a period of 128 s.

tical crustal conductive zones in the central part of the profile. This model (Fig. 4b) can be considered as the final one in the process of the tipper inversion.

Inversion of the Longitudinal Phases of Impedance

The results of the tipper data inversion were used as the initial model in the inversion of the phases of longitudinal impedance (ϕ^{\parallel}). At the preliminary stage of the analysis, we made sure that the dispersion relations between the modulus and the phase of impedance hold in most cases. Therefore, we abandoned using the statistically distorted longitudinal amplitude curves and confined ourselves to the inversion of the phase data alone.

Calculations were carried out for two intervals of periods. First, the inversion of longitudinal phases ϕ^{\parallel} was conducted in the same interval as the inversion of tipplers. However, the phases only slightly vary within this interval, and the result of the inversion turned out to be almost the same as in the case of the tipper inversion; the only distinction is that the contrast of resistivities of the mantle blocks increased. In the extended range of periods (22–4096 s) we obtained the model shown in Fig. 5. In this model, all the main structural elements are identified as distinctly as in the case of the inversion of tipplers. Here, with the use of the longitudinal phases it was possible to correct the shape of the near-vertical conductors (the tipper inversion imaged these structures as overelongated in the horizontal direction). The electrical resistivity of the blocks located above the crustal conductive layer at a depth 10–20 km also decreased. This might be associated with the presence of the other relatively small

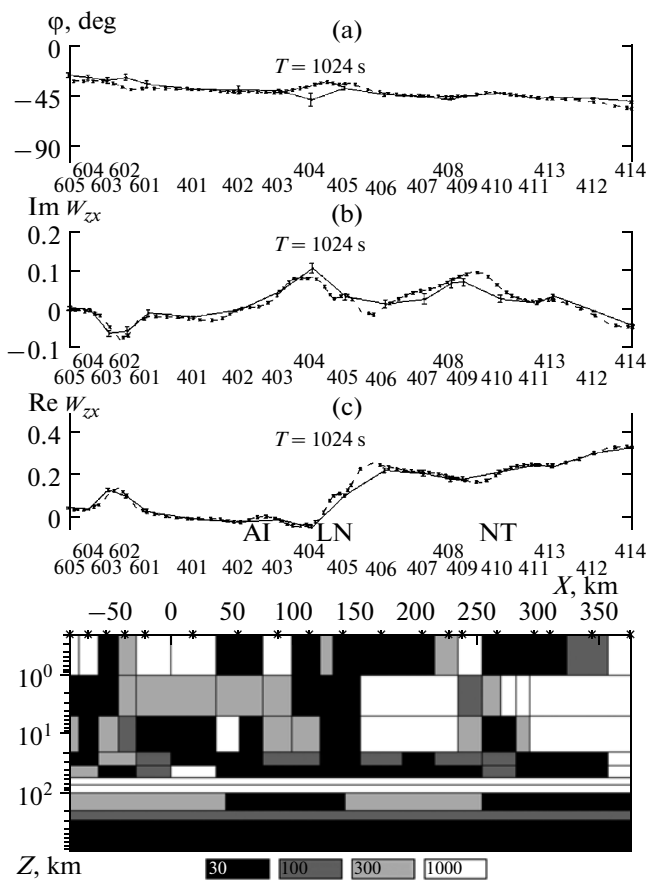


Fig. 6. The final block geoelectric model along the Naryn Line yielded by the sequential partial inversions.

conductive structures in the solid crust above the conducting layer, which appear in such a smoothed form due to the large sizes of the blocks being optimized.

At the same time, we failed to fit the minimum of phase data at periods 256–1024 s at point 404. We recall that in this region of the profile, the dispersion relations were also violated. Possibly, this is connected with the presence of a deep 3D heterogeneity in the geoelectric cross-section, which hampers the 2D selection of data.

Refinement of the Electrical Resistivity of Sediments and the High-Resistivity Part of the Earth's Crust According to the Transverse Impedance Data

The next stage involved the use of the transverse phase and amplitude curves for refining the electrical resistivity of sediments and the upper part of the Earth's crust. The output model of the inversion of longitudinal impedance phases (Fig. 5) was taken as the initial model, and only those blocks were optimized that represented the sediments and the high-resistivity regions of the Earth's crust at a depth of 20 km, as well as the blocks in the upper parts of the Nikolaev Line and the North Tien Shan fault at a

depth of 1 to 5 km. Calculations in the case of H -polarization allowed us to refine the electrical resistivity of the solid crust (in the northern part of the profile it is higher than in the southern part), and also to show that the crustal anomalies of the Nikolaev Line and the North Tien Shan fault are connected with the sedimentary deposits and can serve as the channels for the electric current to flow from the deep conductive layers into the near-surface layer.

4. CONSTRUCTION OF THE GENERALIZED FINAL MODEL AND VERIFICATION OF ITS RELIABILITY

From the results of sequential inversions, a series of models is obtained that exhibit the same common features but somewhat differ from each other in several details. These models were compiled into a generalized final model using the following procedure. The model obtained from the transverse impedance data was somewhat corrected to provide fuller consistency of the entire set of the inverted data. The model resistivities were corrected taking into account the informativeness of the blocks under a permanent monitoring of misfits. The obtained model is presented in Fig. 6.

Next, we tested the significance of the model components in nearly the same way as it was done when constructing the final model in the method of sequential inversions in the EMSLAB experiment [Vanyan et al., 2002]. We removed the individual key structures (the Nikolaev Line, the Atbashi-Inylchek fault, the vertical conducting zone in China, the North Tien Shan fault, and the crustal conducting layer) one-by-one from the model and compared the misfits obtained before and after these changes. We saw that once any of these elements of the model was removed, the misfits appreciably increased. Only with the elimination of the conductive blocks corresponding to the Atbashi-Inylchek fault, the misfits increased insignificantly. The only element not confirmed by this test was the steps in the asthenosphere.

CONCLUSIONS

With the method of sequential partial inversions, it turned out possible to reconstruct the geoelectric section of the medium along the Naryn Line with sufficient reliability. All the main deep structures of the region intersected by the profile, namely, the North Tien Shan fault, the fault zone of the Nikolaev Line, the Atbashi-Inylchek fault, and the northern edge zone of the Tarim Basin, are present in this section. The crustal conductive layer with laterally varying electrical conductivity was confidently identified within the depth interval of 20–55 km. This layer is traced practically along the entire profile, and only on the north of the region it disappears at points 412–414. The data speaking for the heterogeneity of the con-

ductive asthenosphere are obtained, although they need further verification.

It is shown that the MV parameters ($\operatorname{Re} W_{\alpha}$ and $\operatorname{Im} W_{\alpha}$) contain almost complete information about the deep section and their inversion yields the models that are very close to the final generalized model. This result illustrates the conclusions of the work [Berdichevsky et al., 2003] regarding the informational equivalence of the ideal impedance and tipper data in 2D media and agrees with the results of the synthetic MT/MV data inversion in the 2D block models [Varentsov, 2002; 2007]. Thus, the inversion of the tipper data in the complex quasi-2D geoelectric environment can provide a firm basis for further refining estimates yielded by the inversion of the phase impedance responses and selected components of the apparent electrical resistivity.

It is worth noting that the confinement of the model class by the models with fixed geometry and sufficiently large-scale blocks facilitates the stable solution of the inverse problem due to the compactness of the vector of the parameters to be optimized. Here, the choice of the optimized blocks substantially influencing the set of the interpretation data becomes an additional tool stabilizing the solution and allowing for a priori information. Naturally, in this case, the fitting accuracy suffers; however, in practice the stable solution with moderate resolution is preferable to a detailed but unstable one. Therefore, the method of sequential inversion, even in the rather simple form in which it is presented, is of course useful for the solution of an inverse problem in the regions with a complex geoelectric structure.

At the same time, one should not suppose that the almost similar compromise between the stability and the detailedness of the inverse problem's solution cannot be attained either in the simultaneous joint inversion of the entire set of MT/MV data or with the complicated parameterization of the model. For the applied INV2D algorithm, using the robust metrics of the misfit functional, the inconsistencies that are possible in the inversion of the multicomponent data can be efficiently resolved. In [Varentsov, 2002; 2007], the examples of the synthetic data inversion in rather complicated block models are presented, in which the solution's quality of the joint multicomponent inversion is close to the quality of the solution in case of sequential inversion. A striking example of the efficiency of joint multicomponent inversion conducted in the multi-window scanning mode in the INV2D algorithm is the inverse problem's solution for the synthetic data in the extremely complex 2D model reproducing the geoelectric section of the junction zone of the Precambrian and Paleozoic Platforms in the Polish Pomerania [Varentsov et al., 2007].

In the next paper of this cycle, which is now being prepared for publication, we will show in detail the benefits of the application of the new possibilities of the INV2D algorithm mentioned above in the case of

inversion of the set of MT/MV data on the Naryn Line, and how the results of the sequential partial and the joint multicomponent inversions will be compared in the very complex highland conditions of the Central Tien Shan. The preliminary results of this research have been already presented in [Sokolova et al., 2007; 2008]. This analysis will allow us to formulate more specifically the rational strategy for the interpretation of the quasi-2D MT/MV data in the conditions typical for high-mountain orogens.

ACKNOWLEDGMENTS

We are grateful to V.I. Dmitriev for his helpful advices. This work was supported by the Russian Foundation for Basic Research, projects nos. 08-05-00875a and 08-05-00345a.

REFERENCES

1. D. A. Alekseev, N. A. Pal'shin, and Iv. M. Varentsov, "Magnetotelluric Dispersion Relations in a Two-Dimensional Model of the Coastal Effect," *Fiz. Zemli*, No. 2, 84–87 (2009) [*Izvestia, Phys. Solid Earth* **45** (2), 150–166 (2009)].
2. M. N. Berdichevsky and V. I. Dmitriev, *Magnetotellurics in the Context of the Theory of Ill-Posed Problems* (SEG, Tulsa, 2002).
3. M. N. Berdichevsky and V. I. Dmitriev, *Magnetotelluric Sounding of the Horizontally-Homogeneous Media* (Nedra, Moscow, 1991) [in Russian].
4. M. N. Berdichevsky and V. I. Dmitriev, *Models and Methods of Magnetotellurics* (Springer-Verlag, Berlin, 2008; Nauchnyi Mir, Moscow, 2009).
5. M. N. Berdichevsky, V. I. Dmitriev, N. S. Golubtsova, et al., "Magnetovariation Sounding: New Possibilities," *Fiz. Zemli*, No. 9, 3–30 (2003) [*Izvestia, Phys. Solid Earth* **39** (9), 701–727 (2003)].
6. M. N. Berdichevsky and D. O. Pokhotelov, "Violation of the Dispersion Relations in a Three-Dimensional Magnetotelluric Model," *Fiz. Zemli*, No. 8, 3–12 (1997) [*Izvestia, Phys. Solid Earth* **33** (12), 603–612 (1997)].
7. M. N. Berdichevsky, E. Yu. Sokolova, Iv. M. Varentsov, et al., "The Geoelectric Section of the Central Tien Shan: the Analysis of Magnetotelluric and Magnetovariation Responses along the Naryn Geotraverse," *Fiz. Zemli*, No. 8, (2010) [*Izvestia, Phys. Solid Earth* **46**(8), (2010)].
8. V. I. Dmitriev, "Inverse Problems in Electrodynamical Prospecting," in *Ill-Posed Problems in the Natural Sciences* Ed. by A.N. Tikhonov and A.V. Gancharsky (Mir, Moscow, 1987) pp. 77–101 [in Russian].
9. I. G. Kissin and A. I. Ruzaikin, "Relations between Seismically Active and Electrically Conductive Crustal Zones in the Kyrgyz Tien Shan," *Fiz. Zemli*, No. 1, 21–29 (1997) [*Izvestia, Phys. Solid Earth* **33** (1), 18–25 (1997)].
10. W. Siripunvaraporn and G. Egbert, "An Efficient Data-Subspace Inversion Method for 2D Magnetotelluric Data," *Geophysics* **65**, 791–803 (2000).

11. E. Sokolova, M. Berdichevsky, I. Varentsov, et al., "Advanced Methods for Joint MT/MV Profile Studies of Active Orogens: The Experience from the Central Tien Shan," in *Protokoll über das 22 Colloquium "Elektromagnetische Tiefenforschung"* Ed. by O. Ritter and H. Brasse (Dtsch. Geophys. Ges., Potsdam, Germany, 2007) pp. 132–141.
12. E. Sokolova, M. Berdichevsky, I. Varentsov, et al., "Geoelectrical Cross-Section of Central Tien Shan and Geodynamic Implications," in *19th Int. Workshop on EM Induction in the Earth (Extended Abstracts. V. 1)* (Beijing, China, 2008) pp. 203–208.
13. Yu. A. Trapeznikov, E. V. Andreeva, V. Yu. Batalev, et al., "Magnetotelluric Soundings in the Kirghiz Tien Shan," *Fiz. Zemli*, No. 1, 3–20 (1997) [Izvestia, Phys. Solid Earth **33** (1), 1–17 (1997)].
14. L. L. Vanyan, M. N. Berdichevsky, P. Yu. Pushkarev, and T. V. Romanyuk, "A Geoelectric Model of the Cascadia Subduction Zone," *Fiz. Zemli*, No. 10, 23–53 (2002) [Izvestia, Phys. Solid Earth **38** (10), 816–845 (2002)].
15. L. L. Vanyan, Iv. M. Varentsov, N. G. Golubev, and E. Yu. Sokolova, "Construction of Magnetotelluric Induction Curves from a Profile of Geomagnetic Data on Electrical Conductivity of the Continental Asthenosphere in the EMSLAB Experiment," *Fiz. Zemli*, No. 10, 33–46 (1997) [Izvestia, Phys. Solid Earth **33** (10), 807–819 (1997)].
16. Iv. M. Varentsov, "Joint Robust Inversion of Magnetotelluric and Magnetovariational Data," in *Electromagnetic Sounding of the Earth's Interior*, Ed. V. V. Spichak (Elsevier, Amsterdam, 2007), pp. 189–222.
17. Iv. M. Varentsov, "A General Approach to the Magnetotelluric Data Inversion in the Piecewise-Continuous Medium," *Fiz. Zemli*, No. 11, 11–33 (2002) [Izvestia, Phys. Solid Earth **38** (11), 913–934 (2002)].
18. Iv. Varentsov, N. Baglaenko, and E. Sokolova, "EMTESZ-Pomerania WG. 2D Inversion Resolution in the EMTESZ-Pomerania Project: Data Simulation Approach," in *Protokoll über das 22 Kolloquium "Elektromagnetische Tiefenforschung"* Ed. by O. Ritter and H. Brasse (Dtsch. Geophys. Ges., Potsdam, Germany, 2007), pp. 143–150.
19. Iv. M. Varentsov, N. G. Golubev, V. V. Gordienko, and E. Yu. Sokolova, "Study of Deep Geoelectric Structure along the EMSLAB Lincoln Line," *Fiz. Zemli*, No. 4, 124–144 (1996) [Izvestia, Phys. Solid Earth **32** (4), 375–394 (1996)].
20. P. E. Wannamaker, J. A. Stodt, and L. Rijo, "A Stable Finite Element Solution for Two-Dimensional Magnetotelluric Modeling," *Geophys. J. R. Astr. Soc.*, **88**, 277–296 (1987).
21. P. Weidelt, "The Inverse Problem of Geomagnetic Induction," *Zeitschrift für Geophysik* **8**, 257–290 (1972).